

Seepage analysis of the fractured rock mass in the foundation of the main dam of the Xiaolangdi water control project

Yan Xiang¹ · Lin Wang² · Suhua Wu³ · Hui Yuan¹ · Zhanjun Wang⁴

Received: 14 August 2014 / Accepted: 19 April 2015 / Published online: 3 May 2015
© Springer-Verlag Berlin Heidelberg 2015

Abstract The foundation of the main dam in the Xiaolangdi water control project is located on the riverbed with a deep overburden layer. Here, the bed rocks have complex geological conditions and developed faults and fissures. Therefore, seepage within the fractured rock mass of the dam foundation has a significant impact on the safety operation of the dam. Using the fractured rock mass seepage theory, a three-dimensional hydrogeological model of the main dam foundation in the Xiaolangdi water control project is established in this paper which takes into account the distribution of faults and fissures in the foundation. The hydraulic conductivities of the major structures and faults are obtained by back-analyzing the data measured by osmometers embedded in the dam foundation. The model is validated by comparing measured water levels and flow rates with calculated results. On this basis, a sensitivity analysis was made of the different factors affecting seepage in the dam foundation. The following conclusions can be made: (1) Seepage is positively correlated with the

reservoir's water level, but there is hysteresis in the correlation, (2) the concrete cutoff wall in the dam's foundation effectively controls the amount of seepage. Also, an increase in the curtain depth on both banks reduces seepage a certain amount. Furthermore, the right bank is clearly more impermeable than the left bank, (3) the deep-coverage layer of the foundation has a notable influence on seepage. The drainage curtain in the downstream of the dam effectively controls the amount of seepage in the dam foundation and improves the stability of the foundation seepage, (4) faults in the dam's foundation have a significant influence on seepage. If grout-strengthening technology is applied to the curtain, seepage control at the intersection between the curtain and faults should be especially highlighted, (5) the sediment deposit upstream of the dam body has no impact on the quantity of seepage from the dam's foundation, but it does significantly reduce the hydraulic head.

Keywords Xiaolangdi water control project · Fractured rock mass · Dam foundation seepage · Back analysis

✉ Zhanjun Wang
nhriwzj@126.com

Yan Xiang
yxiang@nhri.cn

¹ Nanjing Hydraulic Research Institute, Guangzhou Road 225, Nanjing 210029, China

² Yellow River Water Conservancy and Hydropower Development Corporation, Zijingshan Road 68, Luoyang 471000, China

³ State Key Laboratory of Hydrology-water Resources and Hydraulic Engineering, Xikang Road 1, Nanjing 210098, China

⁴ Key Laboratory of Failure Mechanism and Safety Control Techniques of Earth-rock Dam of the Ministry of Water Resources, Hujuguan 34, Nanjing 210029, China

Introduction

According to the Bulletin of First National Census for Water, China has built 98,002 reservoirs with a total capacity of 932.312 billion m³. In terms of dam type, earth-rockfill dams account for 93 % of these. As far as height is concerned, there are approximately 5000 dams with a height over 30 m and over 32,000 with a height over 15 m. These dams are not only vital engineering measures for temporal and spatial regulation of water resource distribution and water allocation optimization, but also an integral part of the flood control system for rivers. They are

irreplaceable foundations for economic and social development, as well as an inseparable security system for the ecological safety of the environment.

To date, most of these earth-rockfill dams have been in operation for years. Over a long period of running, these dams experience different kinds of special loads and have different typical operating conditions, to different degrees, leading to changes in the working performance of the dam structures and their seepage (Xu et al. 2013). Hence, it is necessary to conduct a retrospective analysis of earth-rockfill dams so that the actual working status of the dams can be evaluated.

Recorded data relating to prototype structure seepage is a comprehensive reflection of the true behavior of the seepage field (Chai et al. 2014). A reasonable computational model has been applied to estimate the optimal values of the hydraulic conductivities of various media in the seepage field (Zhu and Liu 1991). Many substantial studies have been carried out on back analysis of the seepage from dams' foundation rock masses. For example, Wang and Liu (1992) used groundwater levels measured in boreholes to deduce the rock's hydraulic conductivity. Moore et al. (2011) investigated moraine dam seepage using self-potential. Ikard et al. (2014) more recently used self-potential and electrical resistivity tomography surveys together with seismic refraction tomography to determine the hydraulic connection between a reservoir and its seepage zone. Liu et al. (2004, 2005) employed an artificial neural network based on an alternative and iterative algorithm and simulated an annealing Gauss–Newton algorithm to perform back analysis of hydraulic conductivity. Vahid and Ali (2013) introduced a method that integrated artificial neural networks with radial basis function interpolation to model seepage in an earth-fill dam. Ma et al. (2013) performed finite element calculations of seepage from an earth dam considering the effects of an unsaturated region on the seepage field. Zhang et al. (2014) studied the effect of a clay core and grouting curtain using finite element calculations of the seepage. Zhu et al. (1997) combined water levels measured in a pressure tap with finite element analysis to complete a back analysis of the hydraulic conductivities of a dam's body and foundation.

The main objective of this paper is, based on a conceptual hydrogeological model of the dam site zone of the Xiaolangdi water control project, to build a three-dimensional (3D) numerical analysis model for seepage taking into account the fractures, joints, faults, and other disadvantageous geological features of the main dam foundation. Furthermore, the seepage parameters of various materials in the dam site zone will be determined using a numerical inversion technique. Subsequently, the change in the seepage behavior in diverse parts of the dam can be simulated. Also, the reasons for, and locations of, the main

leaks are identified considering conditions such as sediment deposits, the anti-seepage curtain of the dam's foundation, faults, and the varying water level in the reservoir.

Site description

Location of the study area

The Xiaolangdi water control project is located in Mengjin County in western Henan province, China. The dam is approximately 40 km from Luoyang city, and lies in the middle reaches of the Yellow River whose length is 5464 km (Fig. 1). The direction of flow of the Yellow River in the study area is S115–120E. The mean annual precipitation is 650.2 mm. The air temperature ranges from -0.5 to 26.2 °C, and the mean annual temperature of the study area is 13.7 °C.

The main dam of the Xiaolangdi water control project is a rockfill dam with an inclined loam soil core and inner blanket. The elevation of the crest is 281.0 m and the maximum height of the dam is 160 m. In addition, the length and width of the dam crest are 1667 and 15 m, respectively. The maximum width of the dam base is 864 m. The upstream and downstream dam slopes are 1:2.6 (the lower part is 1:3.5) and 1:7.5, respectively. Meanwhile, the upstream cofferdam constitutes a part of the dam. The foundation of the main dam in the Xiaolangdi water control project is located on the riverbed with a deep overburden layer. The bed rock here has complex geological conditions and developed faults and fissures. The maximum depth of the overburden layer reaches 80 m. In designing the Xiaolangdi water control, the principles used for control and the arrangement for foundation seepage amount to: “blocking in foreside and draining on back, water drainage combined with water blockage”. The beneficial effects on the dam foundation of the natural blanket formed by Yellow River sediment has been given full consideration with respect to seepage prevention and different engineering measures have been adopted at the riverbed and both banks. For the riverbed, vertical seepage prevention is mainly used, and this is supplemented with horizontal-seepage prevention. For both banks, curtain grouting was used to prevent seepage.

Geological framework

The stratigraphic units discussed below are listed from the youngest to the oldest, and are defined according to their group and formation names. The stratigraphic unit disclosed in the dam site area is composed of sand, shale, and clay rocks from the Triassic period (*T*), and is distributed in the left bank and riverbed. Sand and shale developed in the

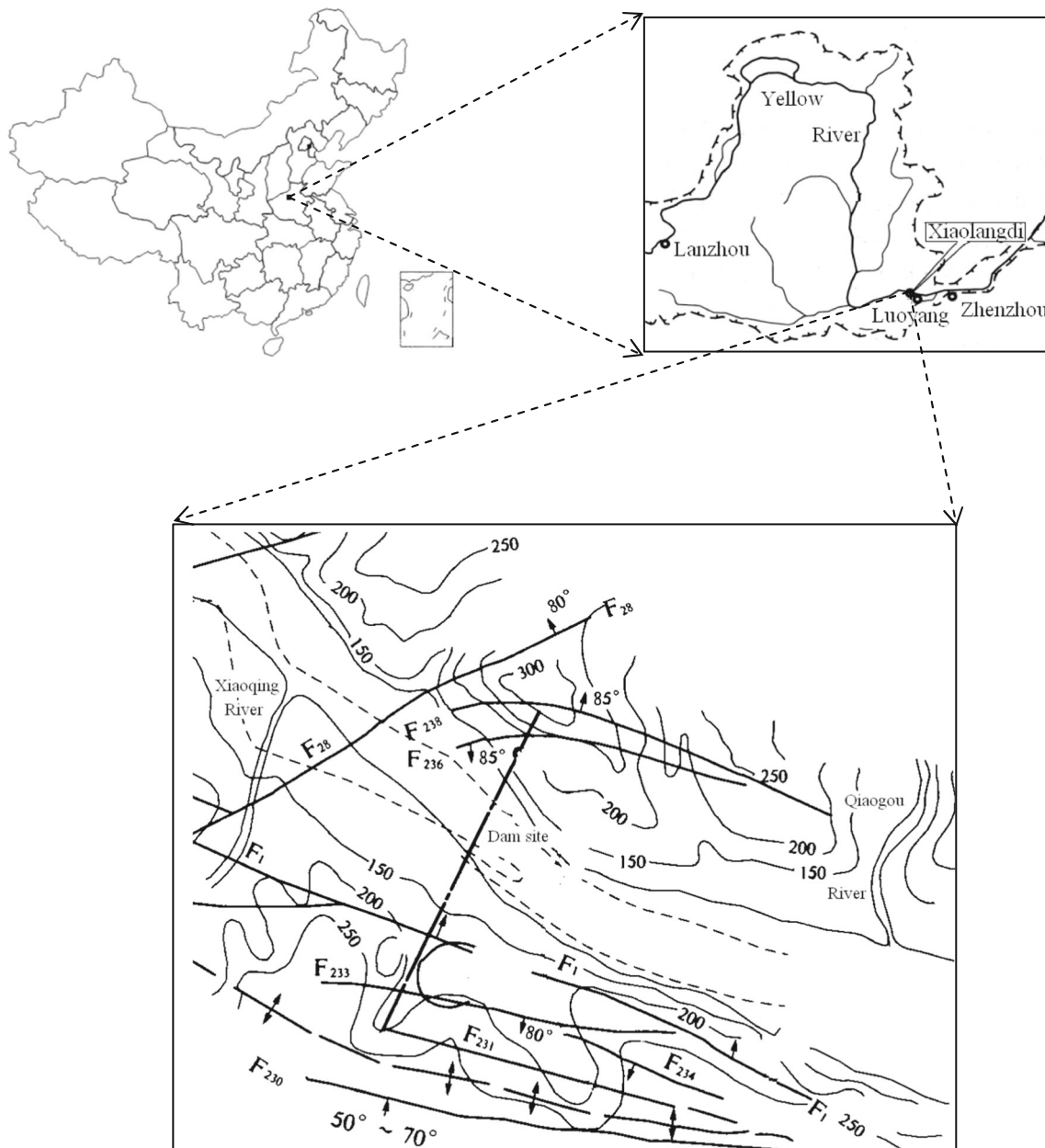


Fig. 1 Location of the study area

Permian period (*P*) are distributed in the right bank. Quaternary sediments form the terrace and river valley with a thickness of 70 m in the dam foundation. A geological cross section along the dam axis is shown in Fig. 2.

According to data from boreholes in the adits, the faults can be divided into two groups. One group is nearly east-west, and the other strikes NE with a high dip angle. Also, the fractures in the study area can be grouped into four types based on their orientations. The first group strikes N30–60E and inclines NW with a dip angle of 75–80°. The second group strikes N70–80E and inclines SE with a dip angle of 56–80°. The third group strikes N20–45W and inclines SE with a dip angle of 75–85°. The fourth group

strikes N55–75W and inclines NE with a dip angle of 80–90°.

Methods

The mathematical model and its solution

Mathematical model

Due to the inhomogeneous and anisotropic nature of the research area, the mathematical model for 3D transient groundwater movement can be expressed in the form:

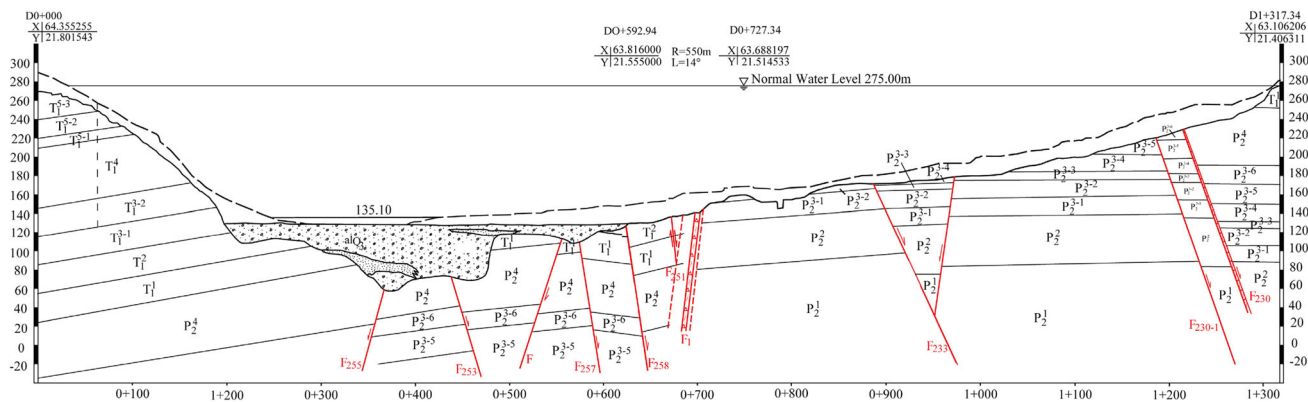


Fig. 2 Geological cross section along the dam axis

$$\begin{cases} S_s \frac{\partial H}{\partial t} = \frac{\partial}{\partial x} \left(K_x \frac{\partial H}{\partial x} \right) + \frac{\partial}{\partial y} \left(K_y \frac{\partial H}{\partial y} \right) + \frac{\partial}{\partial z} \left(K_z \frac{\partial H}{\partial z} \right) \\ + \varepsilon, x, y, z \in \Omega, t \geq 0, \\ H(x, y, z, t)|_{t=0} = H_0, x, y, z \in \Omega, t \geq 0, \\ K_n \frac{\partial H}{\partial n} \Big|_{\Gamma_1} = q(x, y, z, t), x, y, z \in \Gamma_1, t \geq 0 \end{cases} \quad (1)$$

here, Ω is the seepage area, H is the groundwater level of the aquifer (H_0 is the initial value), K_α is the hydraulic conductivity in the direction α (x, y , or z), S_s is the specific storage, and ε is the term for sources and sinks. The secondary boundary conditions are represented by Γ_1 (including the bottom impermeable boundary, lateral flow, or impermeable boundary of the seepage area) and n is the normal direction of the boundary surface. Thus, K_n is the hydraulic conductivity along the normal direction of boundary surface. The quantity $q(x, y, z, t)$ is the flow per unit area through the secondary kind of boundary—inflow is marked as positive and outflow is negative (for an impermeable boundary its value is 0).

Finite element discretization

An algebraic equation for the entire seepage area can be obtained by carrying out finite element discretization of Eq. (1):

$$[G]\{H\} + [P]\left\{\frac{dH}{dt}\right\} = \{F\}, \quad (2)$$

where $[G]$ is the global conductivity matrix, $[P]$ is storage matrix, $\{H\}$ is hydraulic head array of unknown nodes, and $\{F\}$ is a known right-hand side.

Values for dH/dt can be found using a difference method, and Eq. (1) was adopted and an implicit difference scheme. After sorting, the equation can be written as:

$$\left\{ [G] + \frac{1}{\Delta t} [P] \right\} [H_{t+\Delta t}] = \frac{1}{\Delta t} [P] [H_t] + \{F\} \quad (3)$$

Treatment of drainage holes

Drainage holes were set in the mountain on both banks. Their mean hole diameter is 110 mm and they have a spacing of 3 m between them. Combined filters were placed in drainage pores in the fault area and clay rock stratum in the right bank, so as to prevent seepage failure. These drainage holes were processed using bar units.

Calculation of seepage in an element

When the finite element method is used to solve for the seepage field, the partial derivatives of the hydraulic heads at the coordinates of the unit nodes cannot be directly obtained. Therefore, the ‘middle section’ method was used to determinate the amount of seepage (Fig. 3).

Using an 8-node hexahedron unit as an example, the equation for calculation of the amount of seepage through a section S has the form:

$$q = - \int_S K_n \frac{\partial H}{\partial n} ds = -K_n S \frac{\partial H}{\partial n}. \quad (4)$$

In this expression, S is the flow cross section, and n is a unit vector along the positive normal direction of the flow cross section. For an isoparametric unit of the 8-node hexahedron, the mid-section $abcd$ is selected as the flow

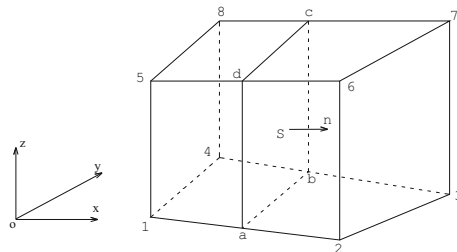


Fig. 3 Diagram showing the calculation of the seepage

cross section S , and S is projected onto the planes yoz , zox , and xoy , which are denoted by S_x , S_y , and S_z , respectively. Therefore, the seepage quantity passing through the mid-section of the unit is:

$$q = -K \left(\frac{\partial H}{\partial x} S_x + \frac{\partial H}{\partial y} S_y + k_z \frac{\partial H}{\partial z} S_z \right). \quad (5)$$

Three-dimensional finite element model for calculation of the seepage of the dam foundation

Calculation area of the model

The calculational area of the model, as the boundary of the contour line at the bottom of the dam, extended for 500 m along the upstream and downstream of the river. It also extended towards the mountains for 200 m on the left bank and 300 m on the right bank (Fig. 4). According to the degree of weathering, the area was divided into three vertical zones, namely, intensely weathered, moderately weathered, and weakly weathered zones. The bottom of the model reached under the confining layer developed in the Permian period (the actual elevation of the bottom was set to -50 m).

Conceptual hydrogeological model

After reservoir impoundment, the zone of reservoir inundation upstream of the dam was selected as the first kind of boundary condition. This condition changes with a change in the storage level of the reservoir. The downstream boundary was taken to be a fixed hydraulic head boundary with a water level of 141.50 m. The rest of the boundary was subject to secondary kinds of boundary condition. The contact between the dam body and dam foundation was assumed to form an impermeable boundary. Also, the

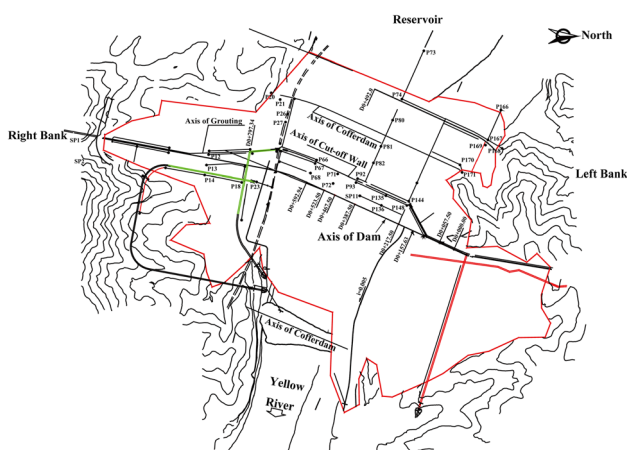


Fig. 4 Calculation area of the model

bottom of the model was a no-flow boundary. The conceptual hydrogeological model is shown in Fig. 5.

Initial material parameters

In the 3D seepage calculation, 4 different materials were considered for the bed rocks of the dam foundation. These represent: the concrete anti-seepage wall of the dam abutment, large-scale faults, the blanket in front of the dam and siltation layer, and the fractured rock mass of the dam foundation. We consider each in turn.

Concrete anti-seepage wall In accordance with preliminary data, the hydraulic conductivity of the dam foundation and concrete anti-seepage wall of the dam abutment was taken to be 1×10^{-8} cm/s. The depth of the dam foundation anti-seepage wall exceeds the cover layer and extends into the bed rock by about 80 m. The suspended curtains are used in the rocks on both banks and the bottom elevations of them are the same as the grouting curtains.

Large-scale faults There are some more developed faults in the dam site zone. Given that these faults greatly influence the seepage of the dam foundation and abutment, the characteristics of the spatial distribution of other faults in the dam site zone were considered in the model. Nine faults in the left bank, right bank, and riverbed of the dam site zone were analyzed in detail. According to the degree of development of the faults and width of the fracture zones, the hydraulic conductivities of the faults were obtained based on the cubic law using the equivalent hydraulic

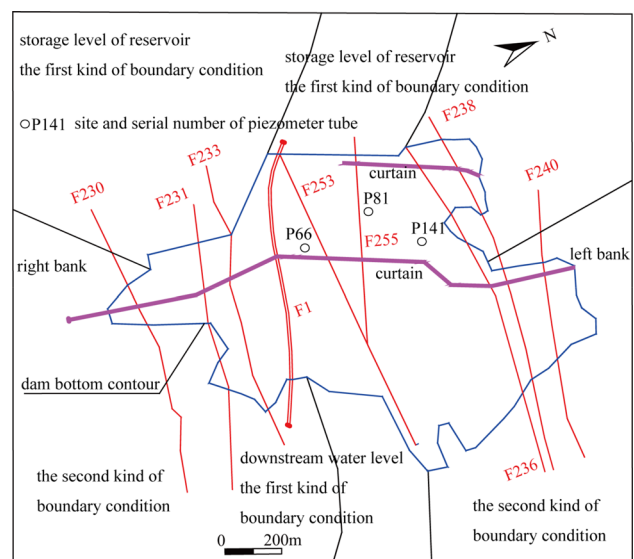


Fig. 5 The conceptual hydrogeological model of the study area

fracture apertures. Among these faults, F_1 , F_{230} , F_{236} , and F_{238} are water-blocking in nature. Moreover, anti-seepage strengthening measurements were preliminarily taken and the hydraulic conductivities were relatively small (Table 1).

Blanket in front of the dam and siltation layer The blanket in front of the dam and siltation layer can prevent seepage. Its hydraulic conductivity was taken to be 1×10^{-5} cm/s.

The bed rock mass In addition to the large-scale faults in the dam site zone, there are some smaller developed faults and joint fissures. These intersected and interconnected with the large faults, forming a fracture network for groundwater transportation. The network presented inhomogeneous and anisotropic characteristics. The rock mass formed several fissure groups through tectonization. As each of the fissure groups contain many fissures, the fractured rock mass can be assumed to be a continuous medium for the purposes of seepage analysis. The flow velocity in the fissures can be assumed to be the velocity of water flow that is continuously filling the entire rock mass. When the fissure medium is assumed to be a continuous porous medium, the anisotropic permeability in the medium can be described using a hydraulic conductivity tensor. When there are several groups of fissures with different attitudes developed in the fractured rock mass, the hydraulic conductivity tensor may be expressed as:

$$K = \sum_{j=1}^n K_{ej} \begin{bmatrix} 1 - \cos\beta_j \sin^2\gamma_j & -\sin\beta_j \sin^2\gamma_j \cos\beta_j & -\cos\beta_j \sin\gamma_j \cos\gamma_j \\ -\sin\beta_j \cos\beta_j \sin^2\gamma_j & 1 - \sin^2\beta_j \sin^2\gamma_j & -\sin\beta_j \sin\gamma_j \cos\gamma_j \\ -\cos\beta_j \sin\gamma_j \cos\gamma_j & -\sin\beta_j \sin\gamma_j \cos\gamma_j & 1 - \cos^2\gamma_j \end{bmatrix} \quad (6)$$

Here, K_{ej} is the equivalent hydraulic conductivity of the j th fissure group, n is the number of groups with fissures developed in the rock mass, and β and γ are the dip direction and dip angle of the fissures, respectively.

If there are fissures with non-equivalent widths and non-equivalent gaps in a group (see Fig. 6), K_e can be calculated using:

$$K_{e1} = \frac{g(b_{11})^3}{12\nu_w L \cos\theta_1} + \frac{g(b_{12})^3}{12\nu_w L \cos\theta_1} + \dots + \frac{g(b_{1n})^3}{12\nu_w L \cos\theta_1} = \frac{g \sum_{j=1}^n (b_{1j})^3}{12\nu_w L \cos\theta_1} \quad (7)$$

where b is the fracture aperture and ν_w is the kinematic viscosity coefficient.

As can be seen from Eq. (6), the hydraulic conductivity tensor is correlated with the selected coordinate system. In different coordinate systems, the unit normal vector for

Table 1 Hydraulic conductivities of main faults in the dam site zone

Position	Fault number									
	F_{240}	F_{238}	F_{236}	F_{255}	F_{253}	F_1	F_{233}	F_{231}	F_{230}	
Mountain on left bank	80–105	Left dam abutment 90–106	Left dam abutment 90–106	Riverbed 105	Riverbed 70–90	Foundation on right bank 285–300	Foundation on right bank 95–102	Foundation on right bank 103–110	Right dam abutment Near EW 52–60	
Strike (°)	80–87	80–85	70–87	75	75	80–85	65	75–90		
Dip angle (°)	0.2–2	1.2–8	1.5–6	0.2	0.2	7–15	0.3	0.1	0.3	
Width of faults (m)	0.01–0.08	$1.0\text{--}3.0 \times 10^{-6}$	$1.0\text{--}3.0 \times 10^{-6}$	$0.005\text{--}0.02$	$0.005\text{--}0.02$	$1.0\text{--}3.0 \times 10^{-6}$	$0.01\text{--}0.02$	$0.001\text{--}0.01$	$1.0\text{--}3.0 \times 10^{-6}$	
Hydraulic conductivity (cm s ⁻¹)										

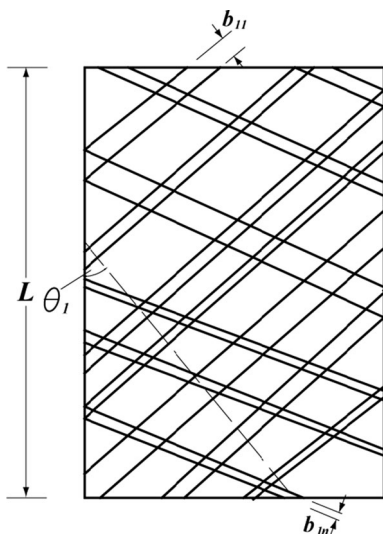


Fig. 6 Fissures with non-equivalent widths and non-equivalent gaps

each fissure plane is different from the direction of the coordinate system. This leads to different hydraulic conductivity tensors. In actual rock mass seepage solutions, if the main axis and main permeability of the hydraulic conductivity tensor can be determined, then the complex form of the water flow control equation in the original problem can be changed. This would greatly simplify the calculation, and yield twice the result with half the effort. A system of orthogonal coordinates $ox_1x_2x_3$ was set up, wherein the corresponding hydraulic conductivity tensor is denoted as \mathbf{K} . As the hydraulic conductivity tensor is symmetric, a new system of orthogonal coordinates $ox'_1x'_2x'_3$ was obtained by rotating the coordinate system. In this way, the hydraulic conductivity tensor was transformed into a diagonal matrix, \mathbf{K}' . In other words, for the new system of orthogonal coordinates $ox'_1x'_2x'_3$, the correlation between \vec{J}' and \vec{v} can be written as:

$$\vec{v}' = -\mathbf{K}'\vec{J}' = -\begin{bmatrix} K_1 & 0 & 0 \\ 0 & K_2 & 0 \\ 0 & 0 & K_3 \end{bmatrix} \vec{J}' \tag{8}$$

where K_1 , K_2 , and K_3 are three main hydraulic conductivities, which correspond, respectively, to the hydraulic conductivities of the rock mass along the three orthogonal directions of the dam site zone, namely K_x , K_y , and K_z .

The geological data indicate that there are 4 groups of fissures developed in the left bank, riverbed, and right bank of the dam site zone. The fissure tendency and angle of tendency can be substituted in Eq. (6) and then the hydraulic conductivity tensor is determined. On this basis, the main hydraulic conductivities K_x , K_y , and K_z can be obtained by rotating the coordinate axis (Table 2).

Back analysis and permeability results

Rock permeability depends on the sizes of the fractures in the rock mass and the spatial distribution of the fracture discontinuities. Expressions for the hydraulic conductivity tensor can reflect the close correlation between the size, direction and spatial position, degree of opening, density, extension length, and connectivity of the fracture discontinuities. To accurately reflect the rock mass in the Xiaolangdi dam site zone, a ‘back analysis’ method is used. The back analysis of the permeability tensors for the riverbed and rock mass on both banks is based on field statistics and analysis of the geometrical parameters of the fracture discontinuities that control the rock seepage. Finally, the hydraulic conductivity tensors are obtained.

Structural plane-controlled back analysis

According to observed and calculated hydraulic heads for some positions in the seepage zone whose coordinates are known (as well as the difference between observed and calculated seepage in the dam foundation), a least-squares method was used to establish the objective function, E . Thus,

$$E(K_j^i) = \sum_{k=1}^M \omega_k \sqrt{(H_k^c - H_k^o)^2} + \sum_{l=1}^N \omega_l \sqrt{(Q_l^c - Q_l^o)^2}, \tag{9}$$

where K_j^i is a parameter to be found (the superscript i indicates the i th sub-area, divided according to the water permeability of the rock mass, and j indicates the j th parameter with $j = 1, 2, \dots, NK$, where NK is the total number of parameters in a certain area. For index i , $i = \text{I, II}, \dots, NNO$, where NNO is the total number of sub-areas.). The quantities ω_k and ω_l are weighting parameters for the k th hydraulic head observation point and l th observed flow, respectively. These obey,

$$\sum_{k=1}^M \omega_k = 1.0, \sum_{l=1}^N \omega_l = 1.0 \tag{10}$$

where M and N are the number of observation points (pores) in the area. The calculated and observed hydraulic heads at the k th observation point are given by H_k^c and H_k^o , respectively. Similarly, Q_l^c and Q_l^o are the calculated and observed values at the l th flow observation point in the area. Obviously, due to the above-mentioned constraining conditions, a group of parameters to be solved can be identified, which leads to the objective function E close to 0.

Table 2 Hydraulic conductivities H of the fractured rocks in the dam site zones

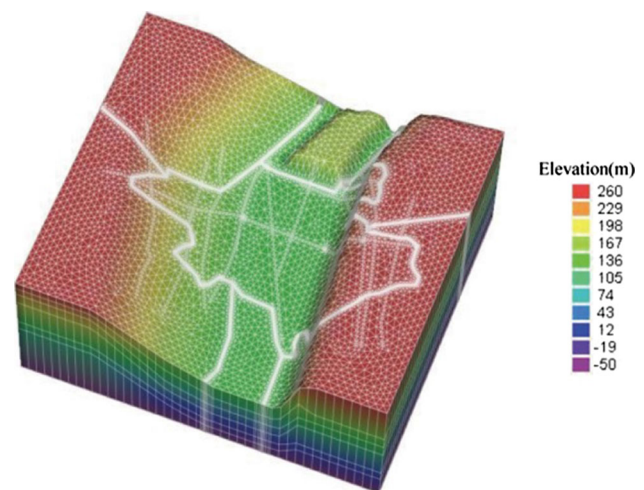
Position	H (cm/s)	Intensely weathered zone	Moderately weathered zone	Weakly weathered zone
Left bank	K_x	$1.51\text{--}4.0 \times 10^{-4}$	$1.0\text{--}5.0 \times 10^{-5}$	$1.0\text{--}5.0 \times 10^{-6}$
	K_y	$1.5\text{--}4.0 \times 10^{-3}$	$1.0\text{--}5.0 \times 10^{-4}$	$1.0\text{--}5.0 \times 10^{-5}$
	K_z	$1.5\text{--}4.0 \times 10^{-3}$	$1.0\text{--}5.0 \times 10^{-4}$	$1.0\text{--}5.0 \times 10^{-5}$
Riverbed	K_x	$1.0\text{--}3.0 \times 10^{-4}$	$3.0\text{--}8.0 \times 10^{-5}$	$3.0\text{--}8.0 \times 10^{-6}$
	K_y	$1.0\text{--}3.0 \times 10^{-3}$	$3.0\text{--}8.0 \times 10^{-4}$	$3.0\text{--}8.0 \times 10^{-5}$
	K_z	$1.0\text{--}3.0 \times 10^{-3}$	$3.0\text{--}8.0 \times 10^{-4}$	$3.0\text{--}8.0 \times 10^{-5}$
Right bank	K_x	$1.0\text{--}3.0 \times 10^{-4}$	$1.0\text{--}5.05 \times 10^{-5}$	$1.0\text{--}5.0 \times 10^{-6}$
	K_y	$1.0\text{--}3.0 \times 10^{-3}$	$1.0\text{--}5.0 \times 10^{-4}$	$1.0\text{--}5.0 \times 10^{-5}$
	K_z	$1.0\text{--}3.0 \times 10^{-3}$	$1.0\text{--}5.0 \times 10^{-4}$	$1.0\text{--}5.0 \times 10^{-5}$

Back analysis results for the rock permeabilities

The permeability of the rock mass in the dam site zone is mainly controlled by the discontinuities. The permeability varies between the left bank, riverbed, and right bank in the dam site zone. A rock mass that controls the groundwater, faults of a certain size, and the structural planes of the joint fissures are considered in the back analysis of the seepage. The intersection point between the dam's axis and the center line of the riverbed is selected as the origin. A coordinate system with the x , y , z axes respectively pointing to the north, west and vertically upward direction is adopted. According to the topography, structure, and permeability, the calculation area was divided into 107,289 nodes and 182,598 elements. This subdivision is shown in Fig. 7.

According to the back analysis model resulting from Eqs. (3) and (9), the hydraulic conductivities of the concrete anti-seepage wall and siltation layer remain the same and the hydraulic conductivities of the faults and rock mass can be obtained through computer calculation (see Tables 3 and 4). Considering the water-blocking properties of F_1 , F_{230} , F_{236} , and F_{238} , the hydraulic conductivity is relatively small. In Table 4, it can be seen that the hydraulic conductivities of the cover layer in the riverbed, above and below the main curtain of the dam foundation, are different. This can be attributed to the effects of the siltation layer, noted to be reasonable.

To confirm the veracity of the 'inversed' model, the seepage from the dam foundation and the groundwater levels in the P81, P141, and P66 observation pores were selected for consideration. The quantity of seepage from behind the dam body starting from May 1, 2011 and ending April 1, 2012 was observed. The observation time for the groundwater levels ran from May 1, 2011 to April 30, 2012. The seepage from behind the dam at these observation time points and the water levels in the observation pores were calculated. The calculated and measured values are shown in Figs. 8 and 9. From these figures, it can be

**Fig. 7** Finite element mesh for the calculation area

found that the calculated seepage from behind the dam is generally smaller than the measured values. When the water level in the reservoir was stable in the range 260.0–265.0 m, the difference between the calculated and measured values is insignificant. The measured data show that when the storage level in the reservoir is comparatively stable, the quantity of seepage from behind the dam is also stable. At the same time, the quantity of seepage measured corresponds to the flow at the corresponding storage level of the reservoir. The calculated water levels agree well with the measured water levels at the 3 observational points. To sum up, the inverse model can effectively reflect the actual situation encountered in the research area. (The hydrogeological parameters obtained from the inversion analysis are also noted to be reasonable).

When the storage level was 260.0 m, the measured quantity of seepage from the dam foundation was 22,975.6 m³/day. This is in good agreement with the calculated value of 22,435.3 m³/day. Contour maps showing the groundwater level are shown in Fig. 10.

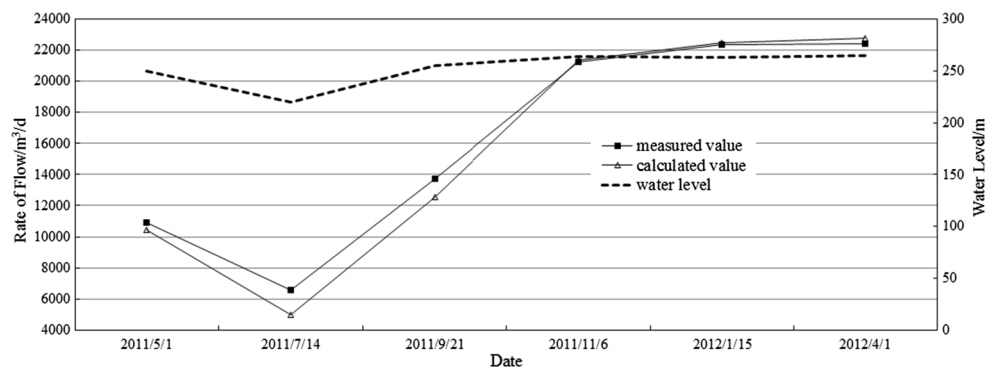
Table 3 Back analysis results for the hydraulic conductivities of the faults in the dam

	Fault number								
	F_{240}	F_{238}	F_{236}	F_{255}	F_{253}	F_1	F_{233}	F_{231}	F_{230}
Position	Mountain on left bank	Left dam abutment	Left dam abutment	Riverbed	Riverbed	Foundation on right bank	Foundation on right bank	Foundation on right bank	Right dam abutment
Hydraulic conductivity (cm s ⁻¹)	0.05	1.5×10^{-6}	1.5×10^{-6}	0.01	0.01	1.5×10^{-6}	0.015	0.005	1.5×10^{-6}

Table 4 Back analysis results for the hydraulic conductivities of the rock mass in the dam site zones

Position	Component	Hydraulic conductivity (cm s ⁻¹)		
		Intensely weathered	Moderately weathered	Weakly weathered
Left bank	K_x	3.0×10^{-4}	3.5×10^{-5}	3.5×10^{-6}
	K_y	3.0×10^{-3}	3.5×10^{-4}	3.5×10^{-5}
	K_z	3.0×10^{-3}	3.5×10^{-4}	3.5×10^{-5}
Riverbed, above main curtain	K_x	2.5×10^{-4}	5.0×10^{-5}	5.0×10^{-6}
	K_y	2.5×10^{-3}	5.0×10^{-4}	5.0×10^{-5}
	K_z	2.5×10^{-3}	5.0×10^{-4}	5.0×10^{-5}
Riverbed, below main curtain	K_x	1.5×10^{-3}	5.0×10^{-5}	5.0×10^{-6}
	K_y	1.5×10^{-2}	5.0×10^{-4}	5.0×10^{-5}
	K_z	1.5×10^{-2}	5.0×10^{-4}	5.0×10^{-5}
Right bank	K_x	2.0×10^{-4}	3.0×10^{-5}	3.0×10^{-6}
	K_y	2.0×10^{-3}	3.0×10^{-4}	3.0×10^{-5}
	K_z	2.0×10^{-3}	3.0×10^{-4}	3.0×10^{-5}

Fig. 8 Curves showing the fitted quantity of seepage for the dam foundation



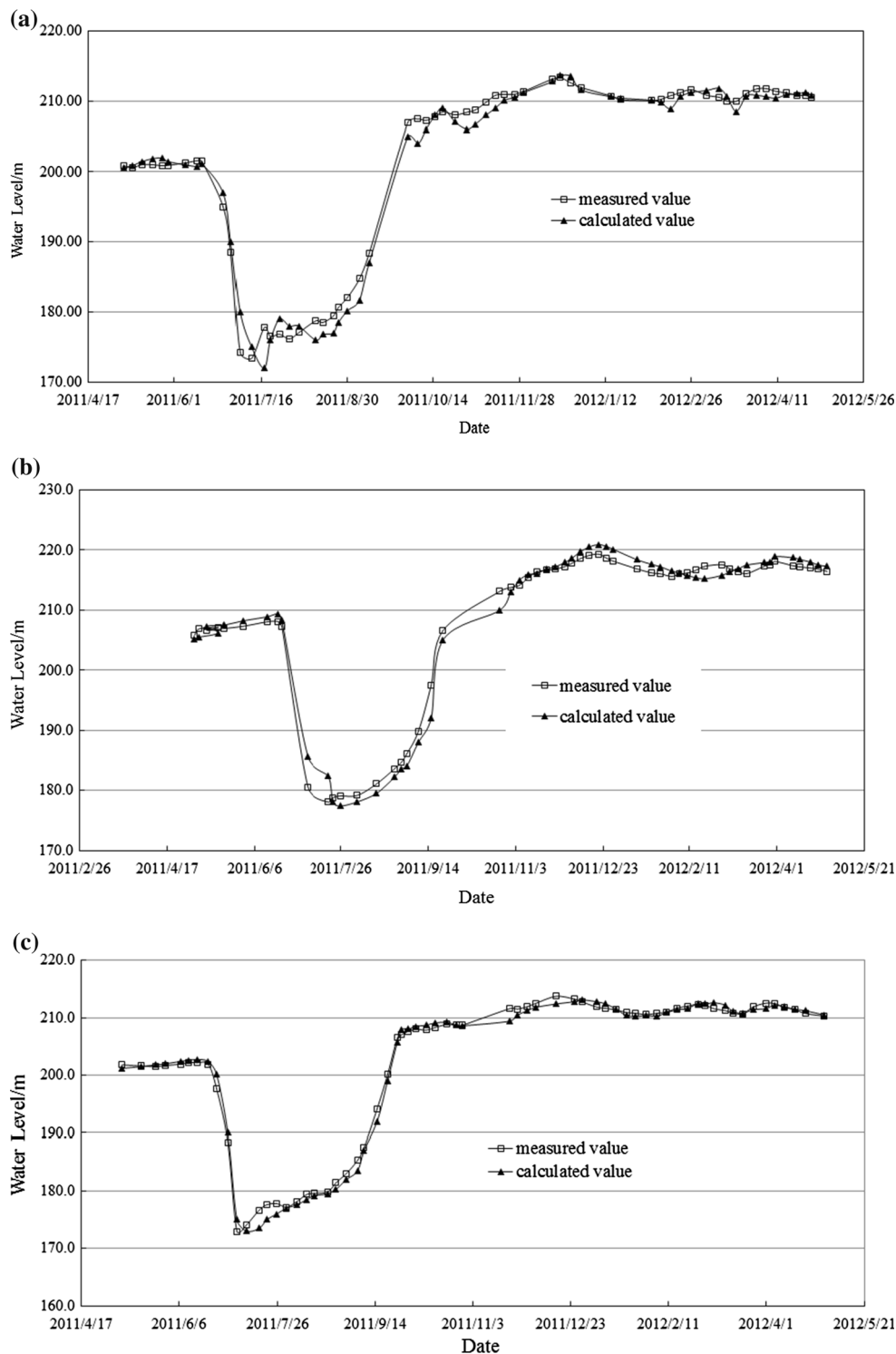
Seepage analysis for the dam foundation rock mass

Using the penetration parameters obtained from the inversion process, the seepage from the dam foundation for different working conditions (between the normal water level of 275.0 m and dead water level of 230.0 m) is predicted using the model. The specific working conditions considered are shown in Table 5. Three main changes in conditions are considered: (1) change in storage level of the

reservoir, (2) change in the curtain’s grouting depth and its hydraulic conductivity (including faults passed by curtain grouting), and (3) effect of the siltation layer upstream of the dam.

If the concrete seepage prevention wall (curtain) is made 25 % less effective (i.e., working conditions 2 and 9), indicating an increase in hydraulic conductivity in the seepage prevention wall, the hydraulic conductivity of the curtain can be calculated using:

Fig. 9 Curves showing the fitted groundwater levels in the dam site zone. **a** P81, **b** P141, **c** P66



$$K_{curtain} = K_{curtain}^0 + (K_{rock} - K_{curtain}^0) \times 25\% \quad (11)$$

where K_{rock} is the average hydraulic conductivity of the rock mass at the curtain and $K_{curtain}^0$ is the hydraulic conductivity when the curtain is completely effective.

Effect of the storage level in the reservoir on seepage

The water level in the Xiaolangdi water control project changes with time, generally falling in the range from 230.0 to 275.0 m. So, the change in seepage quantity for

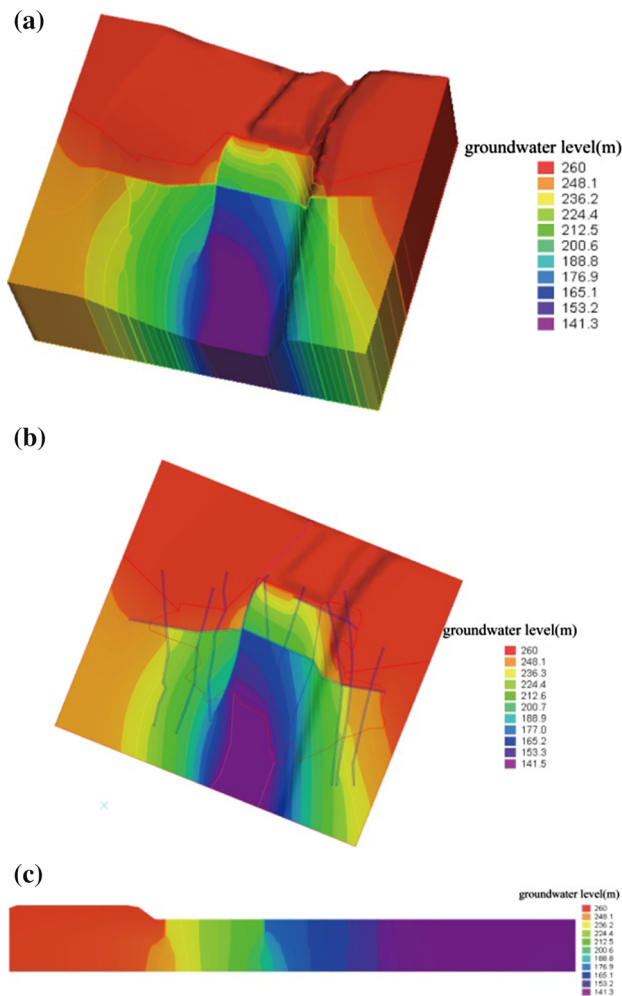


Fig. 10 Contour maps showing the groundwater levels in the dam site zone (storage level of reservoir: 260.0 m). **a** 3D contour map, **b** 2D contour map, **c** contour map for section B–B

the two above-mentioned water levels was considered. As can be seen in Table 6, at the normal water level (275.0 m), the seepage from the dam foundation is 29,533.07 m³/day (working condition 1). Measured data also showed that when the water level was 270.1 m (on November 21, 2012), the observed seepage quantity was 28,953 m³/day, which agrees well with the calculated seepage. When the water level is 230.0 m, a seepage of 19,648.41 m³/day is calculated (working condition 8). It can be inferred from this that as the water level declines, the amount of seepage from the dam foundation is reduced. This is a manifestation of the close correlation between seepage from the dam foundation and the water level of the reservoir. However, the reduction presented is nonlinear. When the water level in the reservoir drops from 275.0 to 260.0 m, the hydraulic head difference is reduced by 15 m and the amount of seepage falls by 7097.77 m³/day. When the water level in the reservoir drops from 260.0 m to

230.0 m, however, the hydraulic head difference falls by 30 m and seepage drops by 2786.89 m³/day.

The measured data indicate that an increase in water level in the reservoir will not immediately induce an increase in the quantity of seepage from behind the dam; there is a time lag between their changes (see Fig. 11a). When the water level in the reservoir is stabilized at a certain value, the seepage from the dam foundation is comparatively stable (Fig. 11b). For example, from August 10 to 20, 2005, the water level in the reservoir varied between 224.53 and 224.95 m, and the corresponding seepage was 20,158.43–20,862 m³/day.

Effect of the concrete prevention wall on seepage

The partial failure of the concrete seepage prevention wall can be seen as equivalent to increasing the hydraulic conductivity. For working conditions 2 and 9, the change leads to the seepage from the dam foundation rising by approximately 66.7 %. This shows that the seepage prevention wall significantly reduces seepage. In addition, we note that in the observation pore P66 the osmometer is in front of the curtain, and P67 and P71 are located behind the curtain. The water level in P66 was thus closely correlated with the water level in the reservoir. However, the change in the water levels in P67 and P71 was insignificant (varying between 137.0 and 138.0 m, see Fig. 12). The difference in the water levels in front of and behind the curtain was about 50 m, indicating an obvious reduction in hydraulic head. This shows that the impervious nature of the seepage prevention wall was effective.

Since the Xiaolangdi water control project came into operation, corresponding engineering measurements on anti-seepage have been performed during different periods for rocks on both banks. More specifically, strengthening of the grouting of the curtain is carried out in areas south of F_1 on the right bank. Grout sealing is adopted for the area in the 120 m range between F_{231} and F_{233} . For the left bank, a row of drilled grout holes is added in the 3[#] and 4[#] grouting footrills, and the preliminary geological exploration holes seal.

After strengthening the grouting of the curtain, seepage from the dam foundation decreased significantly. From the perspective of curtain depth, the bottom elevation of the curtain at the riverbed reached 60.0 m, extending the relative confining layer below the cover layer. The bottom elevation of the curtain at the left bank is about 130.0 m, and the elevation is higher at the right bank than the left. Meanwhile, the relatively impermeable elevations of both banks are distributed between 40.0 and 80.0 m. Hence, the distance between the curtain and the relatively confining layer exceeds 90 m, and the curtain can be categorized as a ‘vertical hanging curtain’. Using the model, predictions are

Table 5 Working conditions for calculating the quantity of seepage from the dam foundation rock mass

Working condition	Description	Water level in the reservoir
1	Inversion parameters include rock mass, faults, and curtain, water level of the reservoir raised to the normal storage level 275.0 m	Normal storage level: 275.0 m
2	Hydraulic conductivity of the concrete seepage prevention wall 25 % less effective	
3	Curtain depth of both banks increased by 50 m	
4	Hydraulic conductivity of dam foundation deep cover increased fivefold	
5	Hydraulic conductivity of all faults increased fivefold at the curtain grouting section and the rest of the faults unchanged	
6	Effect of the upstream siltation layer is ignored	
7	Hydraulic conductivity of the siltation layer decreased fivefold	
8	Inversion parameters include rock mass, faults, and curtain, water level of the reservoir raised to the dead storage level 230.0 m	Dead water level: 230.0 m
9	Hydraulic conductivity of the concrete seepage prevention wall 25 % less effective	
10	Curtain depth of both banks increased by 50 m	
11	Hydraulic conductivity of foundation deep cover increased fivefold	
12	Hydraulic conductivity of all faults increased fivefold in the curtain grouting section and the rest of the faults unchanged	
13	Effect of the upstream siltation layer ignored	
14	Hydraulic conductivity of the siltation layer decreased fivefold	

Table 6 Seepage from different parts of the dam foundation under different working conditions

Working condition	Dam foundation (riverbed)		Left bank seepage (m ³ day ⁻¹)	Right bank seepage (m ³ day ⁻¹)	Left + right bank, percentage of total seepage (%)	Total seepage (m ³ day ⁻¹)
	Seepage (m ³ day ⁻¹)	Percentage of total seepage (%)				
1	17,728.70	60.03	5614.76	6189.61	39.97	29,533.07
2	36,428.38	72.84	6961.18	6621.95	27.16	50,011.51
3	14,565.64	65.90	4257.30	3279.7	34.10	22,102.64
4	23,789.59	60.17	7708.96	8038.75	39.83	39,537.3
5	28,402.45	61.36	8685.16	9200.61	38.64	46,288.22
6	18,011.61	60.38	5648.40	6170.41	39.62	29,830.42
7	17,669.38	59.83	5710.95	6152.32	40.17	29,532.65
8	11,832.27	60.22	3671.59	4144.55	39.78	19,648.41
9	24,246.89	72.98	4559.64	4417.49	27.02	33,224.02
10	9784.66	66.46	2709.45	2228.52	33.54	14,722.63
11	17,835.17	60.15	5668.47	6147.52	39.85	29,651.16
12	20,217.47	63.66	5558.56	5982.48	36.34	31,758.51
13	12,060.17	60.77	3629.86	4155.57	39.23	19,845.6
14	11,832.13	60.22	3671.66	4144.39	39.78	19,648.18

made for a 50 m increase in curtain length at both banks (working conditions 3 and 10). The total seepage from the dam foundation decrease by approximately 5000–7000 m³/day. In other words, the change is equivalent to a daily reduction in seepage of 100–140 m³/day for every 1 m increase in curtain depth. This accounted for

~ 25 % of the current amount of seepage. Seepage at the left bank decreased by approximately 23 %, and that at the right bank by about 45.6 %. The above results show that after strengthening the grouting of the curtain, the decrease in seepage at the right bank is more significant than that at the left bank, assuming the curtain depth increased.

Fig. 11 Curves showing the relationship between the storage level in the reservoir and seepage from the dam foundation. **a** March 10, 2003–June 20, 2004, **b** August 10–November 28, 2005

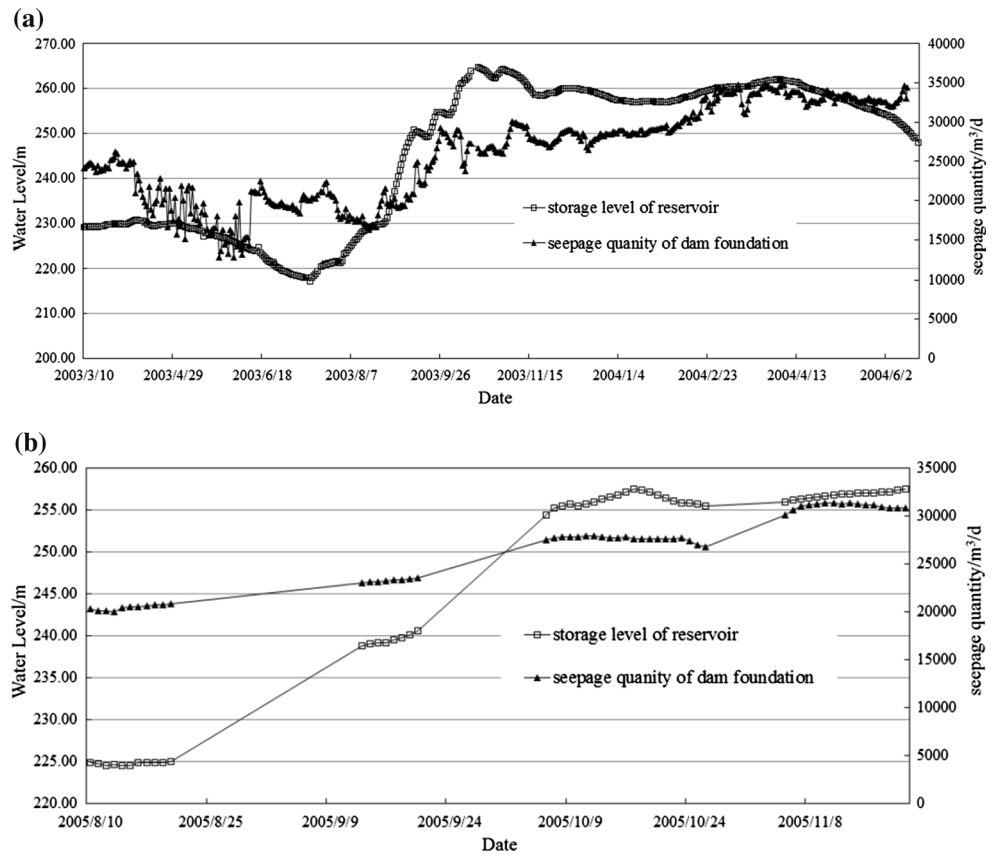
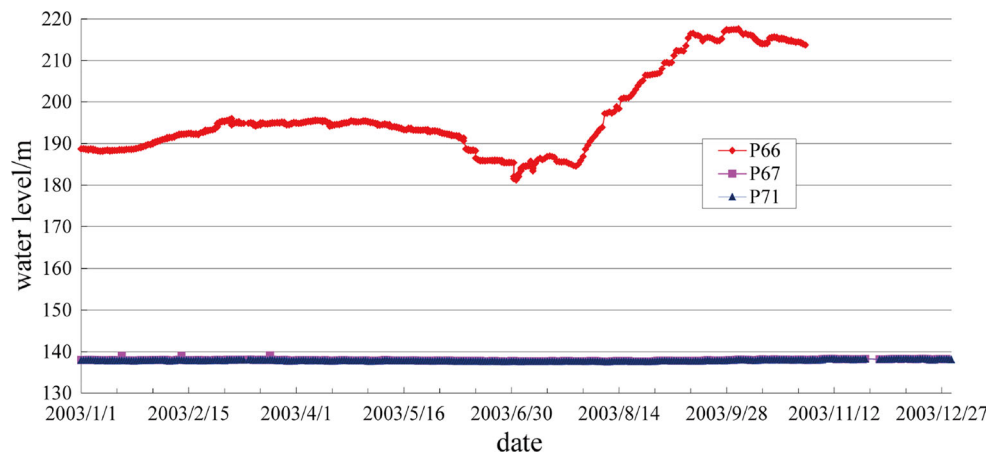


Fig. 12 Time-dependent changes in the groundwater levels in three observation boreholes



Effect of the foundation’s deep cover on seepage

The exploration data show that the thickness of the deep cover in the Xiaolangdi dam foundation is approximately 70 m. Also, the main lithological characteristics can (from top to bottom) be divided into an upper sand and gravel layer, a sand inclusion layer, a bottom sand layer, and a lower sand and gravel layer containing boulders. Due to the different particulate ingredients in the various layers, the permeability of the different layers also presents

remarkable differences. According to the results of 24 pumping tests, the permeability of the upper sand and gravel layer is extremely inhomogeneous. Its hydraulic conductivity is found to be generally around 10.0 m/day. In some pores with high silt content, the hydraulic conductivity is lower, about 1.0 m/day. In the section with a bottom elevation of 100.0–115.0 m, some aerial parts are found to exist. In nine pumping tests, six have a hydraulic conductivity exceeding 45 m/day (more specifically, 225.58, 171.7, 101.74, 84.17, 80.83, and 45.27 m/day).

This layer is a high permeable layer, and is distributed in the bottom sand layer in the quirk of the bed rock in the riverbed. It is continuously distributed from the curtain axis of the dam seepage prevention curtain to a distance 200 m in the downstream direction of the dam axis, with a wide distribution area. From the curtain axis of the seepage prevention wall to the dam axis, the sand layer is 12–18 m thick. The thickness of the sand layer is 4–18 m below the dam axis. Its hydraulic conductivity is 5.97–0.21 m/day.

Above the sand layer, there is a strongly permeable sand and gravel layer, with aerial phenomena, which has a hydraulic conductivity of 225.58–80.89 m/day. Its elevation is generally distributed in the range 100.0–115.0 m. Below the sand layer, there is a sand and gravel layer containing boulders and with a hydraulic conductivity varying between 94.49 and 70.98 m/day. It is also a high permeable layer. There is a low permeable layer between them. Therefore, the hydraulic conductivity of the cover layer mainly varies between 10^{-1} and 10^{-3} cm/s. For a cover layer with a high silt content, the hydraulic conductivity drops to between 10^{-3} and 10^{-4} cm/s.

During normal operation of the dam, the thickness of the siltation layer in the upstream of the dam is about 50 m. Under the effects of the hydraulic head difference between the upstream and downstream of the dam, some of silt might be brought to the cover layer as a result of the groundwater flow. This leads to a rising silt content in the cover layer and decreases hydraulic conductivity. The silt is mainly distributed upstream of the primary seepage prevention curtain. Downstream of the primary seepage prevention curtain, it is difficult for the silt to enter the downstream coat layer (through the relatively confining layer) because the curtain extends into the bed rock. Hence, when the model parameters are adjusted, the hydraulic conductivities differ in the upstream and downstream cover layers of the riverbed (see Table 4). This is consistent with the order of magnitude of the hydraulic conductivities calculated from the field pumping tests. Under such circumstances, the hydraulic conductivity of the coat layer of the dam curtain downstream of the riverbed is increased (working conditions 4 and 11). Therefore, during the process of groundwater flow, fine particles in the coat layer may be brought out, forming small seepage channels in the cover layer. In other words, the hydraulic conductivity of the cover layer increases.

From Table 6, it can be seen that when the hydraulic conductivity of the dam foundation deep cover increases 5-fold, the total seepage quantity rises by about 10,000 m³/day (equivalent to $\sim 30\%$). It can thus be deduced that the foundation's deep cover greatly influences the foundation's seepage quantity. Therefore, it is appropriate to arrange drainage holes in the downstream to reduce water pressure. This measure can prevent the removal

of fine particles from the cover layer during groundwater flow. Furthermore, it effectively controls the quantity of foundation seepage and improves the stability of seepage from the dam foundation.

Effect of faults on seepage from the dam foundation

There are many developed faults and fissures in the dam foundation. These intersect and interconnect, allowing transportation of the groundwater in the fracture network (Fig. 13). The development of the faults and fissures presents some general characteristics: (a) Most of the faults and fissures have developed along the river's direction (Fig. 13a), that is, they are basically parallel to the river. This facilitates seepage in the foundation. The permeability of the faults along the river is large. If the direction of flow of the river was to cross the faults at large angles, or vertically with respect to the faults, the quantity of seepage from the dam foundation would be decreased. (b) There are many fissures and faults with steep angles. According to Fig. 13b, the angle of inclination of most faults exceeds 60° , and some even approach 90° . These steep inclination angles reduce the underground resistance encountered when transportation occurs in the fissures. At the same time, the flow velocity accelerates, and the water exchange interaction between the faults and fissures is enhanced. Furthermore, faults and fissures with steep angles deteriorate the blocking ability of the grouting section, leading to channels which concentrate groundwater seepage.

Using working conditions 5 and 12, the effects of 9 faults on the quantity of seepage from the foundation in the dam site zone were analyzed. These faults (e.g., F_{240} , F_{255} , F_{253} , F_{233} , and F_{231}) are large in scale and have wide crush zones. As can be seen from Table 6, when the hydraulic conductivity of the curtain intersecting with faults is increased fivefold, the total seepage from the dam foundation rose by about 55%. That of F_{240} , F_{255} , F_{253} , F_{233} , and F_{231} increased by 98%. The total seepage due to other faults (e.g., F_1 , F_{238} , F_{236} , and F_{230}) rose by approximately 2%. These faults intersect with faults and fissures with smaller sizes at different positions. The intersection forms a possible seepage channel in the dam foundation. Hence, when strengthening the curtain grouting, seepage prevention between curtain and faults should be given special attention. As most of the faults have a steep angle of inclination, arranging a few inclined holes is necessary during grouting to achieve satisfactory seepage prevention effects.

Effect of the siltation layer on seepage

The siltation layer in front of the dam and the inner blanket constitutes a sound horizontal-seepage prevention system. Using the model, predictions were made for the following

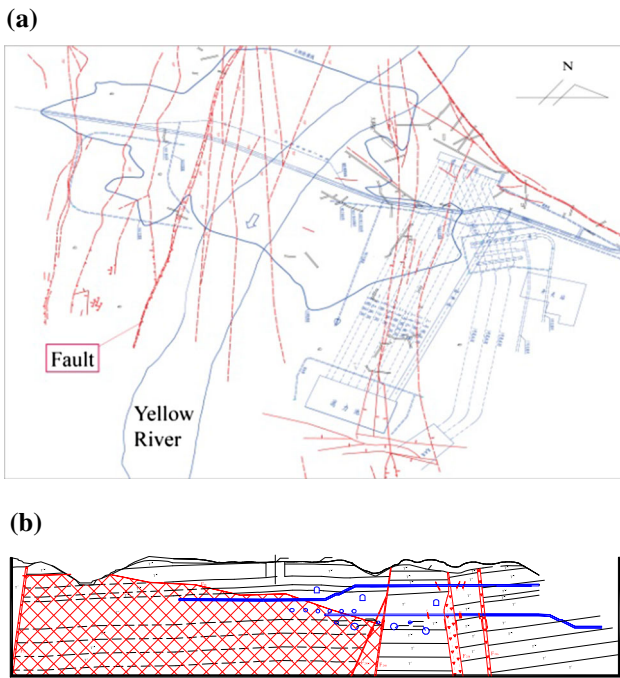


Fig. 13 The fault distribution in the dam site zone. **a** Plane map, **b** cross section

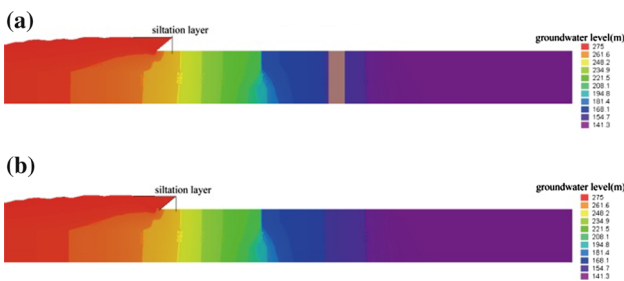


Fig. 14 Front and back hydraulic head changes in the siltation layer for different working conditions. **a** Working condition 1, **b** working condition 7

circumstances: absence of a siltation layer (working conditions 6 and 13), and occurrence of a siltation layer with a hydraulic conductivity 5 times smaller than the set value of 1×10^{-5} cm/s (working conditions 7 and 14). The results show that when a siltation layer is not present, the total seepage from the dam foundation increases by 1 %. If the hydraulic conductivity of the siltation layer is reduced fivefold, the total seepage barely changes (see Table 6). This demonstrates that the existence of a siltation layer only has a small impact on the seepage.

Although the horizontal-seepage prevention system (comprising the siltation layer and inner blanket) has an insignificant impact on seepage from the dam foundation, the calculation results indicate that it significantly reduces the hydraulic head (Fig. 14). For example, under working condition 1 (a storage level of 275.0 m in the reservoir and

seepage prevention in the form of a natural siltation layer), a hydraulic head of 255.0 m is predicted. This decrease of 20 m accounts for 14.9 % of the total hydraulic head (difference in hydraulic head between the upstream and downstream). However, if the seepage-preventing natural siltation layer is not taken into account (working condition 6), the reduction in hydraulic head is about 9 m, accounting for 6.7 % of the total hydraulic head. If the hydraulic conductivity of the siltation layer is reduced fivefold, the reduction in the hydraulic head is about 24 m, i.e., 17.9 % of the total hydraulic head (working condition 7). If the hydraulic conductivity of the siltation layer is 1×10^{-6} cm/s, or the thickness of the siltation layer is increased, the reduction in hydraulic head exceeds 20 %. This is essentially identical to that actually observed. Hence, the hydraulic head reduction is correlated with the thickness of the siltation layer and hydraulic conductivity. At the same time, because of the different in-built positions of the osmometers, the calculated hydraulic heads present certain differences as a result of the heterogeneous anisotropy of the siltation layer.

Analysis of seepage for different parts of the dam site zone

The preliminary monitoring data, and the reasons why seepage occurs from the dam foundation, suggest that seepage mainly arises from the riverbed of the dam foundation—seepage from both the left and right banks is less significant. This is also considered in the back calculation of the parameters. According to Table 6, under different working conditions, the amount of seepage from the left and right banks accounts for approximately 36.8 % of the total seepage. Of this, the contribution made by the seepage from the right bank is slightly larger than that from the left bank. Seepage from the riverbed accounts for the other 63.2 % of the total seepage. This is consistent with measured seepage quantities. Due to the fact that some of the monitoring points used to determine seepage were damaged, the calculated seepage values are actually smaller than the measured values.

Conclusions

1. According to monitored water levels measured at osmotic pressure points and the measured flow from the dam foundation, the hydraulic conductivities of the faults and rock mass in a dam site zone were determined. A three-dimensional numerical simulation method was used and a ‘back analysis’ approach used. The model was verified through comparison of the measured water levels and flows with calculated values.

2. The amount of seepage from the dam was found to be positively correlated with the water level in the reservoir. In other words, seepage from the dam foundation also increases significantly as the water level in the reservoir increases. There is also a time lag between the changes. Therefore, the observed seepage does not reflect the seepage quantity corresponding to the reservoir water level when there are sudden rises and falls in the reservoir water level. If the reservoir water level is stable, then seepage from the dam foundation is also stable. The calculation results demonstrate that when the reservoir water level is between 230.0 and 275.0 m, the total seepage quantity is about 20,000–30,000 m³/day.
3. The concrete seepage prevention wall of the dam foundation effectively controls the quantity of seepage. A 25 % fall in the seepage prevention effect of the wall corresponds to an increase in seepage quantity of approximately 66.7 %. Additionally, an increase in the curtain depth on both banks can reduce the seepage quantity to a certain degree—the seepage prevention effect on the right bank is better than that on the left bank.
4. The deep cover of the dam foundation significantly affects the seepage quantity. If the hydraulic conductivity of the dam foundation deep covers increases fivefold, the total seepage quantity increases by approximately 30 %. It is observed that the drainage curtain arranged downstream of the dam is able to lower the water pressure and prevents the removal of fine particles from the cover layer induced by groundwater flow. Thus, the drainage curtain effectively controls seepage from the dam foundation and improves the stability of the seepage.
5. Faults in the dam site zone also greatly affect the quantity of seepage. If the hydraulic conductivity of the curtain intersecting with faults is increased fivefold, the total seepage from the dam foundation rises by about 55 %. Among the faults, F_{240} , F_{255} , F_{253} , F_{233} , and F_{231} are responsible for 98 % of the effect, while the other faults (e.g., F_1 , F_{238} , F_{236} , and F_{230}) account for about 2 %. Hence, when strengthening the grouting of the curtain, prevention of seepage at the intersection of the curtain and faults should be given special attention. As most of the faults have steep inclinations, inclined holes set during slip casting can be used to effectively decrease the permeability of the fault crevices.
6. The siltation layer upstream of the dam had no effect on the seepage quantity from the dam foundation. In the absence of a siltation layer, the amount of seepage from the dam foundation rises by 1 %. Meanwhile, if the hydraulic conductivity of siltation layer is decreased fivefold, then the total seepage from the dam foundation remains unchanged. This suggests that the

impact of the siltation layer on seepage can be neglected. From the foregoing discussion, the siltation layer in front of the dam significantly reduces the hydraulic head. Furthermore, the magnitude of the reduction is correlated with the thickness of the siltation layer and hydraulic conductivity. The calculation results show that if the hydraulic conductivity of siltation layer reduces 100 times, the hydraulic head is reduced by over 20 %.

7. The simulation results indicate that the seepage from both banks collectively account for about 36.8 % of the total amount of seepage. The remainder (63.2 % of the total) is due to leakage from the dam foundation.

Acknowledgments This work was supported by the National Natural Science Foundation of China (Grant No. 51179108) and the Special Fund for Public Welfare Industry of Ministry of Water Resources of China (Grant No. 201501033).

References

- Chai XD, Shen ZZ, Nie BS (2014) Study on the anti-seepage reinforcement scheme of earth-rock dam for Changli Reservoir. *Adv Mater Res* 904:389–392
- Ikard SJ, Rittgers J, Revil A et al (2014) Geophysical investigation of seepage beneath an earthen dam. *Groundwater* 53:238–250
- Liu XS, She CX, Zhang LJ (2004) Back analysis of seepage with ANN based on alternative and iterative algorithm. *Chin J Rock Eng* 23(9):1470–1475 (in Chinese)
- Liu XS, Zhou CB, Zhang LJ (2005) Application of neural network based on simulated annealing Gauss-Newton algorithm to seepage back analysis. *Rock Soil Mech* 26(3):404–408 (in Chinese)
- Ma CC, Li SY, Wu LY (2013) The research on the finite element seepage calculation of earth dam considering the effect of unsaturated region. In: Fourth international conference on digital manufacturing and automation (ICDMA). IEEE, Qingdao, pp 1532–1534
- Moore JR, Boleve A, Sanders JW (2011) Self-potential investigation of moraine dam seepage. *J Appl Geophys* 74:277–286
- Vahid N, Ali B (2013) Integration of artificial neural networks with radial basis function interpolation in earthfill dam seepage modeling. *J Comput Civil Eng* 27(2):183–195
- Wang SJ, Liu JX (1992) Determination of hydraulic conductivity model for concrete foundation by optimum inversion. In: international symposium on monitoring technology of dam safety, vol. 10
- Xu H, Huang B, Rao XB et al (2013) Research on new dam structure for high earth core rockfill dam on thick overburden. *IACGE* 2013:316–323
- Zhang HH, Wang CY, Gong AM (2014) Seepage analysis of plane finite element on clay core dam of Laojunshan. *Adv Mater Res* 838:1637–1640
- Zhu YM, Liu WT (1991) Optimal estimation method for back analysis of hydraulic conductivity. *Chin J Geotech Eng* 13(4):71–76 (in Chinese)
- Zhu YM, Zhang LJ, Wu Y (1997) Back analysis of coefficient tensor of permeability for fractured rock mass. *Chin J Rock Eng* 16(5):461–470 (in Chinese)